Scoping and Screening Complex Reaction Networks Using Stochastic Optimization

E. C. Marcoulaki and A. C. Kokossis
Dept. of Process Integration, U.M.I.S.T., Manchester M60 1QD, U.K.

A systematic methodology to target the performance of chemical reactors with the use of stochastic optimization is presented. The approach employs a two-level strategy where targets are followed by the proposition of reactor configurations that match or are near the desired performance. The targets can be used for synthesis and retrofit problems, as they can provide the incentives to modify the operation, and ideas in developing the reactor design. The application of stochastic optimization enables confidence in the optimization results, can afford particularly nonlinear reactor models, and is not restricted by the dimensionality or the size of the problem.

Introduction

The area of reactor network synthesis currently enjoys a proliferation of contributions in which researchers from various perspectives are making efforts to develop systematic optimization tools to improve the performance of chemical reactors. The contributions reflect on the increasing awareness that textbook knowledge and heuristics (Levenspiel, 1962), commonly employed in the development of chemical reactors, are now deemed responsible for the lack of innovation, quality, and efficiency that characterizes many industrial designs. The new methods focus on a systematic and thorough consideration of the available options and employ technology in the form of superstructures, optimization techniques, and a variety of graphical methods.

Thanks to Aris, the importance of mathematical methods in optimizing reactors has been exemplified early enough with the application of dynamic programming for the estimation of optimal operating conditions in CSTR cascades (1960) and the development of graphical techniques for single reversible reactions in PFRs (1961). Around the same time, a set of brilliant contributions by Horn (1964) provided the basis of material that later emerged as attainable-region (AR) approaches. Dyson and Horn (1967) developed graphical tools for optimal temperature control schemes, feed distribution profiles along a PFR and catalyst minimization problems (Dyson and Horn, 1969). In these early days, separate groups made attempts to consolidate options and alternatives within comprehensive reactor structures (Ng and Rippin, 1965;

Jackson, 1968; Ravimohan, 1971). Optimization approaches initially addressed fixed reactor structures. Examples include the work of Paynter and Haskins (1970), and Chitra and Govind (1981, 1985a,b). The first studies of comprehensive structures should be attributed to Achenie and Biegler (1986, 1988, 1990), who employed existing representations (Jackson, 1968; Ng and Rippin, 1965) to launch optimization techniques in the form of NLP methods.

Kokossis and Floudas (1990, 1991, 1994) first introduced the idea of a reactor network superstructure modeled and optimized as an MINLP formulation. Though general and inclusive, their representation did not follow previous developments, but made an effort to facilitate the functionalities of the MINLP technology with the synthesis objectives. Mainly to scope, optimize and analyze the reaction process, Kokossis and Floudas replaced detailed models with simple though generic structures, enough to screen for design options and estimate the limiting performance of the reaction system. In the same vane, dynamic components have been replaced by CSTR cascades. A superstructure of generic elements (ideal CSTRs and PFRs) was postulated to account for all possible interconnections among the units. The representation was modeled and optimized as a MINLP model.

Around the same time, Glasser et al. (1987) retrieved and extended the insightful methods of Horn (1964). They presented graphical procedures supported by simple and illustrative examples. Their approach requires the graphical construction of the convex hull of the problem and helps to exemplify the need for a systematic and general methodol-

ogy. Though useful in two dimensions, in higher dimensions their developments face both graphical and implementation problems. Indeed, higher dimensions assume the employment of numerical procedures through which the construction of the convex hull represents an NP-hard problem. Though fundamental limitations appear evident, persistent efforts to extend the graphical methods have appeared in the literature (Hildebrandt et al., 1990; Hildebrandt and Glasser, 1990; Glasser et al., 1992, 1994; Feinberg and Hildebrandt, 1997; Price et al., 1997; Glasser and Hildebrandt, 1997; Hopley et al., 1997; Nisoli et al., 1997; McGregor et al., 1999; Godorr et al., 1999).

A more promising direction has been pursued by Biegler and coworkers. The motivation has been to instill better guarantees in the optimization efforts by exploiting ideas and rules established in the construction of the AR. Applications presented in this area include the work by Balakrishna and Biegler (1992a,b) and Lakshmanan and Biegler (1994, 1996, 1997), and involved mathematical programming applications in the form of NLP and MINLP formulations. Optimal control formulation has been presented by Rojnuckarin et al. (1996) and Schweiger and Floudas (1999). Hildebrandt and Biegler (1994) presented a review of the attainable region approaches and suggested areas for future development of the concept.

Targeting Objectives and Optimization Technology

Whether mathematical programming can reap benefits from the attainable region developments is not for this article to discuss. Instead, the discussion of this section is devoted to the synthesis objectives perceived for the design problem in question. From a practical viewpoint, the nature of a useful approach for reactor network synthesis should primarily account for:

(i) Solid performance limits for the reaction system

(ii) The systematic development of layouts that approach this performance.

The first part, the *targeting stage*, is particularly useful provided there is enough confidence in the optimization results. Since the design equations of chemical reactors feature a significant amount of nonconvex terms, the importance of confidence assumes a significant place. From a targeting viewpoint, layouts near the targets are considered equally important. Consequently, the construction of envelopes, the development of attainable regions, and the identification of "correct" reactor sequences that trace the borders of graphical developments are not part of the approach. Solutions in the interior of the attainable region make valid options provided they remain close to the targets.

Unfortunately, many researchers who overlook borders and optimal solutions assume a relative meaning in reactor design. The reaction kinetics typically involve significant uncertainties and approximate models that give little justification for a strict emphasis on the optimum. In this context, the development of a CSTR−PFR−CSTR−PFR−CSTR−PFR layout as an "optimal" configuration represents an academic exercise of limited interest. A single CSTR, seemingly inferior by 1 or 2%, can feature operational advantages and even

prove a better choice in the form of an industrial back-mixed reactor.

The type of information required from the targeting stage naturally relates to the results one can obtain with the application of the stochastic optimization approach. In particular, this work applies simulated annealing (Kirkpatrick et al., 1983), which is a statistical cooling optimization technique that generates a biased random search and employs Monte Carlo simulations under a variable probability schedule. Chemical engineering applications include work for heat-exchanger networks (Dolan et al., 1987, 1989, 1990; Nielsen et al., 1994; Muller and Kokossis, 1995; Athier et al., 1997a,b, 1998), multiproduct batch (Das et al., 1990; Xia and Macchietto, 1997), and noncontinuous plants (Patel et al., 1991), separation and reaction (Floquet et al., 1994; Marcoulaki and Kokossis 1995, 1996a,b; Cordero et al., 1997), utility networks (Maia et al., 1995), flow-sheet optimization (Painton and Diwekar, 1995; Chaudhuri and Diwekar, 1996, 1997), and molecular design synthesis (Marcoulaki and Kokossis, 1998).

Simulated annealing (SA) is based on a randomized evolution of states through stepwise modifications. The acceptance of intermediate states is based on the amount of improvement they bring to the objective (Metropolis et al., 1953) and the annealing temperature, β. New states evolve as the annealing temperature is updated via cooling schedules that account for the asymptotic convergence of the stationary points between successive choices (Aarts and van Laarhoven, 1985; Sorkin, 1991; Gidas, 1985).

The second part, the *screening and scoping* stage, is accommodated by superstructure developments. The importance of screening is exemplified in a variety of recent research studies and can be accomplished by either a stepwise approach (Kelkar and Ng, 1998) or a simultaneous search (Shah and Kokossis, 1997; Marcoulaki and Kokossis, 1998; Briones and Kokossis, 1998a,b,c, 1996). The idea of presenting SA applications against (non)linear or mixed-integer (non)linear programming (that is, LPs, NLPs, MILPs, and MINLPs) methods accounts for the fact that the stochastic methods have made very limited use of the superstructure schemes employed by the mathematical programming developments. The superstructures are exhaustive representations of synthesis options and an essential background for the formulation of the mathematical programming methodology (Grossmann, 1985). However, because they account for general and compact schemes with a focus on optimization, they maintain their value beyond the scope of mathematical programming. This section explains the use of superstructure within the context of an annealing process.

Let us consider the reactor network superstructure of Figure 1. Its stream network establishes interconnections among the superstructure units, and the selection of streams defines exhaustive combinations of layouts. Figure 2 illustrates conventional and novel designs obtained as special cases. Referring to the annealing process, each one of these cases represents a *design instance* or a *state* of the stochastic process. Consequently, the superstructure accounts for the domain of instances or the *superstate* model the annealing is searching. The evaluation of the states can employ shortcut or black-box models (for example, confidential, in-house developments of industrial groups or Fortran-based simulation models) and can be assessed on the basis of an optimization objective (cost,
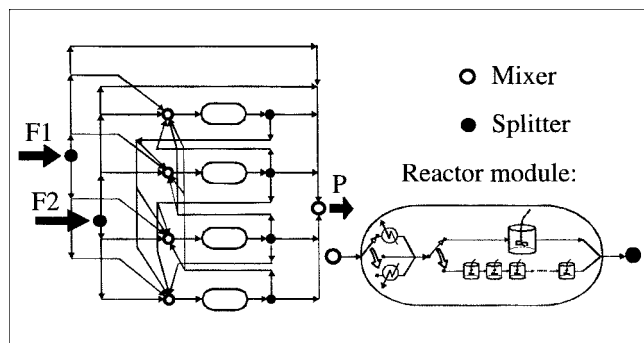
Figure 1. Reactor superstructure with 4 units, 2 feeds, and 1 product.

Figure 3. State-to-state transitions: units.

profit, etc.) of the most general type. The transition from one state to another directly relates to the building components of the superstructure, and includes:

• *Structural elements* with transitions to account for changes from one reactor type to another, introduction of new units, elimination of units, and modifications of the units' size and capacity.

• *A stream network* with transitions to include the introduction of new stream connections (based on existing structural units), elimination of existing streams, and modifications of mass and volumetric flow rates.

Figure 3 illustrates some structural moves, with the base case design being the CSTR of Figure 3a: a new reactor can be added (PFR in Figure 3b) or the type of the existing one can be changed (Figures 3c and 3d). Figure 4 illustrates stream network moves. Starting from the PFR–CSTR scheme of Figure 4a new streams are introduced (Figures 4b and 4c), and parallel structures can be revealed (Figure 4d). In non-isothermal superstructures, additional moves account for the elimination of heat-exchanger units and the changes in their capacities.

Starting from some initial state, a transition process can be developed in the form of a Markov chain that can be searched and assessed within an annealing schedule. The convergence of the annealing algorithm will provide a stochastically optimal design. The superstructure can be used to define states and facilitate a systematic evolution of potential layouts. Perturbation probabilities can reflect on preferences and biases
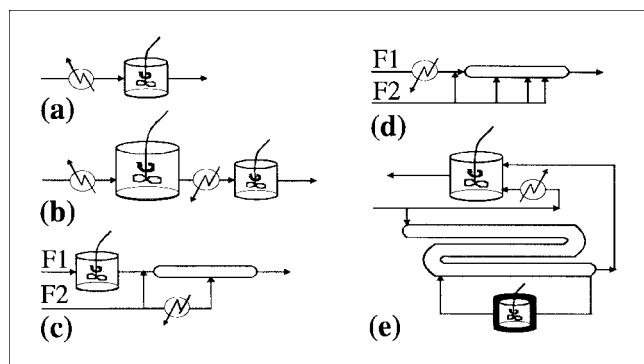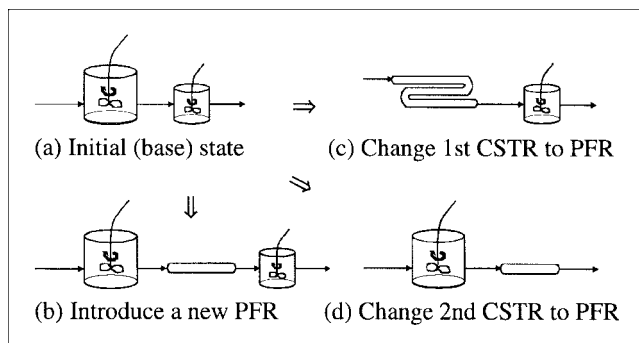
related to the particular application. The evolution of states and the Markov process will have to be repeated for a number of runs before the result is declared an optimum. The use of larger or smaller Markov chains will provide the degree of confidence behind the optimization task. The confidence about the optimum can be quantified from the variations in the optimization results from the different stochastic runs.

In summary, the application of stochastic optimization within a superstructure scheme can provide

• Design targets that exploit features of the superstructure
• Confidence levels for the optimization results obtained
• Structural and operational alternatives with performance close or exactly matching the targets.

Unlike their deterministic counterparts, the targets are reliable performance limits associated with quantifiable confidence. Due to the nature of the stochastic approach, there is a multitude of alternatives found with a performance that matches or remains close to the targets. Most of these alternatives make useful design ideas for the practitioner and an excellent initial point for rigorous calculations (for instance, CFD models) to verify the promised features and account for even more.

Proposed Design Framework

The previous section explains the use of superstructure schemes with a stochastic optimization search. The development of isothermal and nonisothermal reactor network superstructures was addressed by Kokossis and Floudas (1990, 1994), who provided details for the units and connectivities of

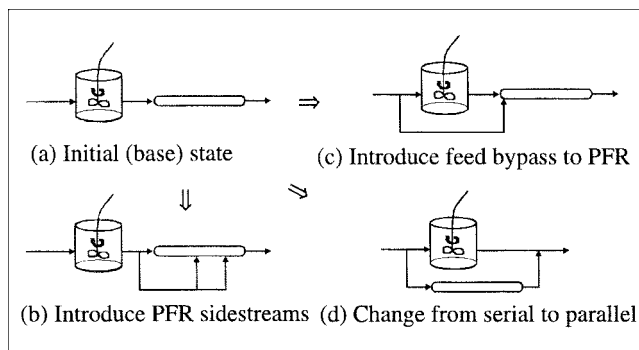Figure 2. Conventional and novel designs arising from Figure 1.

Figure 4. State-to-state transitions: streams.

these networks. The stochastic search over the superstructure schemes is described in the form of the following stages:
- Development and evolution of states
- Assessment and acceptance criteria
- Cooling schedule and convergence.

Development of states

On the grounds of an initial or current state (base state), the approach randomly generates new states that involve new units and streams. New and base states are both instances of the reference structure, which accommodates various flow, mixing, and temperature control patterns. Each state is identified with respect to its type of process units, the operating characteristics of its units, and its stream network.

The *units* refer to reactors and heat exchangers. The types of reactors include CSTRs and PFRs (both isothermal and adiabatic). The types of heat exchangers include heaters and coolers. The operating characteristics of the reactors consist of their volumes and their residence times. The operating characteristics of the heat exchangers involve their heat-transfer area. Each reactor unit is directly connected to a potential heat exchanger for feed preheating/cooling. The reactor–exchanger arrangement is preceded by a mixing point and is followed by a splitting point. The entire mixing–heating–reaction–splitting scheme composes a process *module*. Additional splitters and mixers relate to the initial feed(s) and final product(s), respectively.

The *stream network* defines connectivities between the units, the feeds, and the products. The flow rates of streams are also defined within the state representation and satisfy constraints on feasibility of material balances. Units that set up the base case make the *existing* units of the state and feature a stream network of *existing* and *nonexisting* connections. These are the *active* streams that represent potential links among the existing units. *Inactive* streams consist of connections that involve units not currently employed.

Evolution of states

The state evolution is carried through a probabilistic set of moves that relate to each state element that was described earlier. The evolution is developed through perturbation probabilities assigned to each class of moves. The moves apply to the process units and the stream network. The former consist of structural and operational modifications. Opera-
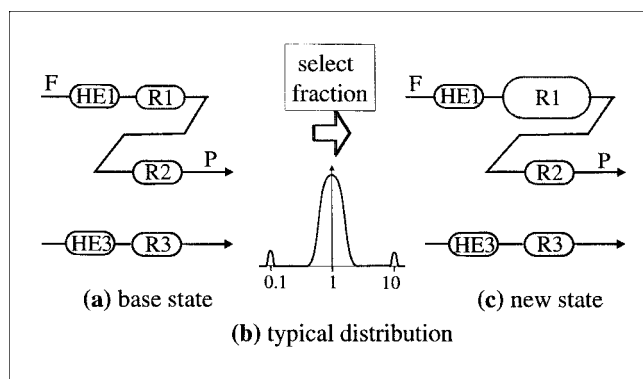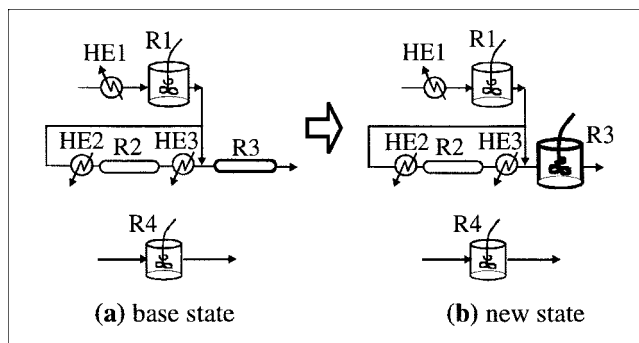

Figure 6. Unit reshuffling.

tional moves include *sizing*, and structural moves include *reshuffling, contraction*, and *expansion*. Moves associated with the stream network relate to stream *shifting*. These moves are described as follows:

1. *Sizing* applies to all existing units, namely reactors and heat exchangers. The move involves the selection of: an existing process unit M_i; a volume or area fraction to adjust the unit size. Applied on the base case of Figure 5a, the sizing operation considers options among the available units $\{HE_1, R_1, R_2\}$. Assuming reactor $\{R_1\}$ is selected, a volume fraction is chosen based upon a given distribution, say that of Figure 5b. The layout of Figure 5c is obtained as a result of the move. Note that for nonisothermal applications the area of the heat exchanger can be altered in the same way as the volume of reactor units.

2. *Reshuffling* refers to changes in the types of existing units. The move involves the selection of: an existing unit M_i of type A; an alternative type B, and change of M_i from A to B. This operation is illustrated in Figure 6, where an existing reactor, namely a PFR, is selected and changed to a CSTR. In nonisothermal applications, moves to switch heaters to coolers, remove existing heat exchangers, or introduce new ones can be addressed in the same context.

3. *Contraction and expansion* refer to changes in the number of existing units. If the unit is a reactor, then the accompanying heat exchanger is removed/introduced along with the reactor module.

The operation of *contraction* eliminates existing units through the following steps: selection of an existing unit M_i; adjustment of the stream network to isolate the unit; and elimination of the unit along with its input/output streams.
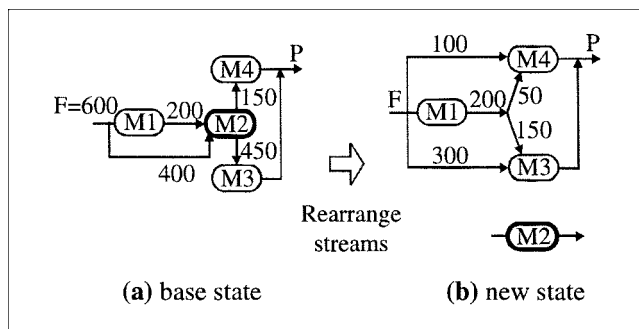

Figure 5. Unit sizing.

Figure 7. Contraction operation.

Figure 8. Expansion operation.

Figure 7 illustrates these 3 steps. As reactor module $\{M_2\}$ is "deleted," its streams are proportionally spread away from the remaining units toward the new state in Figure 7b.

The operation of *expansion* introduces nonexisting units through the following actions: selection of a nonexisting unit M_i; selection of an existing stream (k, l); and expansion of the stream network and inclusion of unit M_i through (k, l). The operation is illustrated in Figure 8. Stage (i) selects M_4, stage (ii) selects (s_F, m_2), and stage (iii) yields the layout of Figure 8b.

Contraction and expansion are profound changes, as they shrink and enlarge the base structure. Both alter the active mixers and splitters, which account for the grand canonical features of the problem (Dolan et al., 1987, 1989, 1990).

4. *Shifting* applies to all active process streams and involves the selection of: an existing splitter, s_i; two active mixers m_j and m_k, so that link (i, j) corresponds to an existing connection; and a load fraction to be shifted from (i, j) to stream (i, k). The load fractions are splitting fractions of the current flow rates. In their limit, they can give rise to new (active) streams or eliminate existing connections. Consider the flowsheet of Figure 9a. Step (i) selects s_1 from the available splitters $\{s_F, s_1, s_2\}$. From the available mixers $\{m_1, m_2, m_P\}$ only $\{m_2, m_P\}$ combine existing connections. Stage (iii) will change the flow rates of (s_1, m_P) and (s_1, m_2). At the limit one of these connections can be removed.

Note that, for the move set to be efficient one should avoid overlapping between moves. For instance, adding or deleting a stream connection should be checked against the status of units before and after the action. That is, the involved connection should not introduce a new process unit or remove

Figure 9. Stream shifting.

Figure 10. Implementation flowchart of the simulated annealing algorithm.

an existing one. Additionally, deleting or adding units should not affect connectivities within the current network state.

Implementation Framework

A simplified flow diagram of the implementation framework is presented in Figure 10. The user identifies the desired components of the superstructure (reactors, connections, etc.) and the perturbation matrix. The optimization requires initial values for the annealing temperature (β) and the chain length (N). The length of the Markov chain per β-interval and the minimum β quantify the termination criteria for the inner (chain) and the outer (temperature) search loops.

Initialization

The cooling process is based on the completion of a fixed number of moves. This number accounts for the chain length (N). The chain iterations terminate after $(N/2)$ accepted moves, or (N) total moves. The final annealing temperature is fixed to a very small value and the optimization process terminates once this bound is satisfied. The initial β value is set for 10 times the maximum expected deviation in the objective (Aarts and van Laarhoven, 1985). *A priori* estimates of the deviation provide safe values for β.

The perturbation probabilities are presented on Table 1. The assignment of probabilities has not considered the physical system, namely the practicalities or prior knowledge of trade-offs. In practical applications, better distributions should consider these issues.

Table 1. Perturbation Probabilities

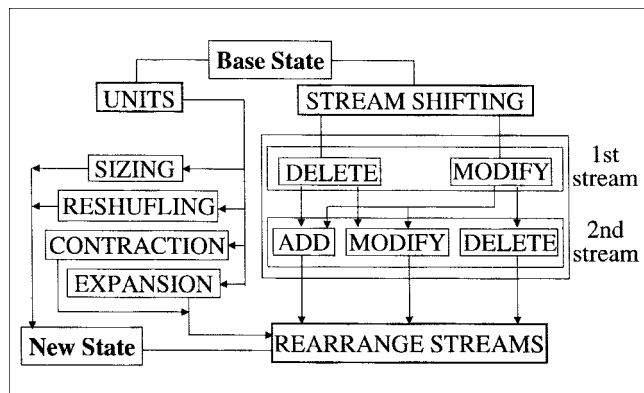| Module Moves	Probability %	Stream Moves	Probability %
Module over stream	60/40	Stream over module	40/60
Unit reshuffling	20	Delete stream	30
Contraction	20	Add new stream	30
Expansion	20	Modify stream load	40
Unit sizing	40	Feed over process	40/60
CSTRs over PFRs	50/50	streams	

Figure 11. Flowchart for move selection.

The probabilities of Table 1 refer to the move selection process illustrated on Figure 11. Perturbation probabilities are assigned to each one of the steps, and they bias the available actions. Stream shifting is regarded as a separate option, thus distinguishing between *stream* and *process unit* moves. For the stream network, additional steps control the selection of feed over process-originated streams. For the units, further biases can be considered in adding, deleting, or modifying reactors of different types.

Evaluation and assessment

For each state, simulation runs converge mass and energy balances. The balances are first converged for total flow rates (linear system), followed by composition and energy balances.

Flow-rate Balances. The variables include stream flow rates, and splitting fractions are introduced as fixed parameters provided by the stochastic moves. Finally, the solution of the linear system is checked against user-specified bounds. If the bounds are not satisfied, a restoration step resets streams and restores bounds. This stage helps in identifying infeasible modifications to the base case, and speeds up the calculation of the nonlinear balances that follows next.

Component and Heat Balances. The variables include reactant and product compositions and temperatures at the outlet of reactors and mixers. The equations include:
- Component mass and heat balances around the mixing points
- Heat balances around the heat exchangers
- Component and heat balances around the reactor units (PFRs are simulated as CSTR cascades)
- Reaction rate and heat equations.

The nonlinear set of equations is solved using NEQLU (Chen and Stadtherr, 1981). To facilitate and speed up the solving process, the algorithm considers only the units affected by the move, rather than the entire network. Identification of the disturbed part follows simple concepts from set theory applied on the network connectivity matrix. This matrix stores existing stream connections as logical variables. The square of the matrix provides second-order connectivities, the cube provides third-order connectivities, and so on. Thus, it becomes possible to identify the units associated with the streams or reactors modified during the current move. This identification step significantly decreases the size of the nonlinear system, yielding on lower CPU times for the entire stochastic run.

Cooling schedule and convergence

According to the Aarts and van Laarhoven (1995) cooling schedule, the annealing temperature, β, is updated after a certain number of iterations have been completed:

$$\beta^{k+1} = \left[1 + \ln(1+\delta) \cdot \beta^k / \Delta E_{\max}(\beta^k)\right]^{-1} \cdot \beta^k,$$

where k represents the current temperature interval, and δ is a statistical cooling parameter that controls the speed of the annealing process. The maximum energy deviation, $\Delta E_{\max}$, at each temperature level, β^k, is given by

$$\Delta E_{\max}(\beta^k) = E_{\max}(\beta^k) - E_{\min},$$

where $E_{\max}(\beta^k)$ is the maximum energy value over β^k, and $E_{\min}$ is the minimum energy.

Conventional annealing schedules use the approximation:

$$\Delta E_{\max}(\beta^k) \cong 3 \cdot \sigma(\beta^k).$$

This approximation does not require knowledge of the minimum energy, but becomes invalid for short chains, while longer chains require long relaxation times and slower annealing (Aarts and van Laarhoven, 1985).

The cooling schedule proposed here updates the annealing temperature, β, using $\Delta E_{\max}$ by

$$\Delta E_{\max}(\beta^k)$$
$$= \min\{\langle E(\beta^k)\rangle + 3 \cdot \sigma(\beta^k), E_{\max}(\beta^k)\} - E_{\min}^*,$$

where $E_{\min}^*$ is the minimum value of the passing objective. The standard deviation can be evaluated by (Johnson and Kotz, 1970)

$$\sigma(\beta^k) = \sqrt{\sum_{i=1}^{t^k} \left(\langle E(\beta^k)\rangle - E_i(\beta^k)\right)^2 / (t^k - 1)},$$

where t^k is the number of iterations over β^k.

During the early stages of annealing the standard deviation, σ, dominates the cooling, while the algorithm establishes good approximations for $E_{\min}^*$. The minimum energy term is constantly updated, and it prevents the system from freezing at some locally optimal value by using information on better solutions accumulated during the search. The new schedule allows shorter chains and higher values for parameter δ. In the examples presented, δ is optimized to $\delta \approx 0.12$ and compares favorably with conventional runs that feature $\delta \approx 0.05$. This allows the system to start from very high temperatures and quickly cool down to the "freezing" temperature, where it spends most of the computational time (Kirkpatrick et al., 1983). On the basis of the evidence accumu-

Table 2. Design Bounds and Increments

Variable	Characteristic	Value
Reactor residence time	Maximum	10^4 s
Reactor residence time	Minimum	10^{-4} s
Reactor residence time	Increment	10^{-4} s
Stream flow rate	Maximum	—
Stream flow rate	Minimum	5% of feed
Stream-splitting fraction	Increment	0.05

lated by the following examples, the new schedule has increased the CPU time by 4 to 5 times.

Illustration Examples

The examples illustrated here emphasize the targeting and scoping stages discussed in the synthesis objectives. In all cases, stochastic experiments are presented with respect to the Markov chains involved, the number of required experiments, and the standard deviation observed in the optimization. The examples address conventional problems (Van de Vusse-Denbigh reaction), as well as problems with highly nonlinear kinetics and stiff models. Unless it is stated otherwise, the superstructure consists of four isothermal reactors. Design bounds and increments employed throughout the optimization search are shown on Table 2.

Example 1: Denbigh reaction

The reaction scheme involves five components and is described by:

$$2\,A \xrightarrow{\ 1\ } B, \quad B \xrightarrow{\ 2\ } C, \quad A \xrightarrow{\ 3\ } D, \quad 2\,B \xrightarrow{\ 4\ } E$$
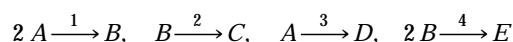
with the following kinetics:

$$R = [\, R_1, R_2, R_3, R_4 \,]$$
$$= \left[-k_1 \cdot x_A^2, -k_2 \cdot x_B, -k_3 \cdot x_A, -k_4 \cdot x_B^2 \right],$$

where $k_1 = 3.0$ lt/mol·s; $k_2 = 0.06$ s^{-1}; $k_3 = 0.6$ s^{-1}; $k_4 = 0.3$ lt/mol·s; $x_i = C_i/C_A^0$ (lt denotes long ton). The feed is 100 lt/s and consists of A (6.0 mol/lt) and D (0.6 mol/lt). The objectives include the maximization of (1) the selectivity of A to B, and (2) the conversion of A to B. The different design stages are described as follows.

Targeting Stage. The maximum selectivity is found to be 1.304, and the maximum exit concentration of B is 0.2528 mol/lt. The results of each stochastic run required an average of 120 CPU·s on a HP 9000-C100 workstation. The statistical experiments included 10–40 runs. Figure 12a illustrates targeting results for maximum selectivity against different Markov chains. The results are presented based on *average values* from the stochastic experiments; *optimal values* are apparently higher. Figure 12b illustrates the development of the standard deviation of the experiments against the Markov chain. Chains shorter than 16 result in high deviations; longer chains indicate converged experiments with standard deviation smaller than 1%. Each point of these figures corresponds to a sample of 40 different runs that use (1) different initial design structures, and (2) different initialization seeds.
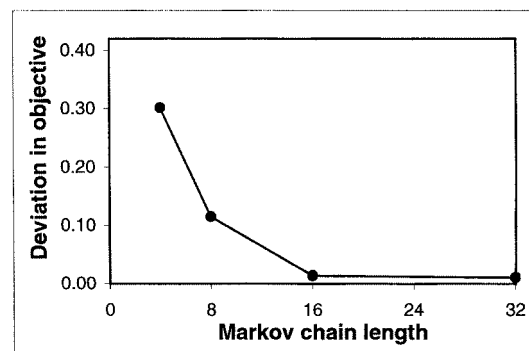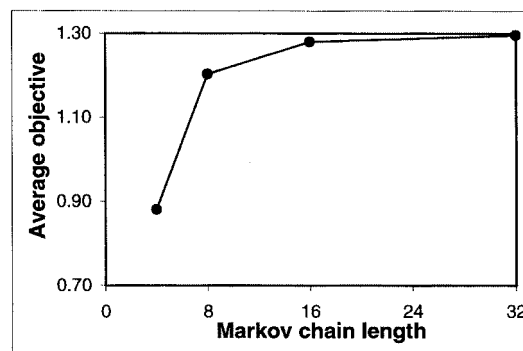

Figure 12. Results for Example 1 (i).

Figure 13 illustrates the robustness of the approach to initialization. The 40 runs of Figures 12a and 12b are presented with respect to the initial designs employed: PFR, CSTR, 2 CSTRs, and CSTR–PFR. The results clearly demonstrate that
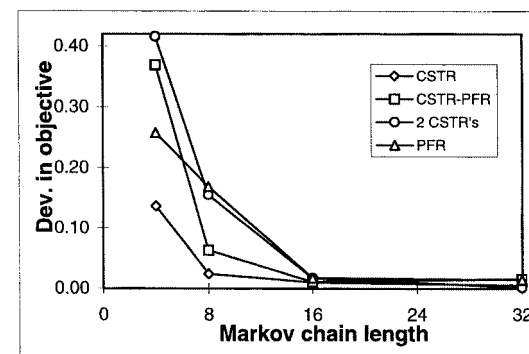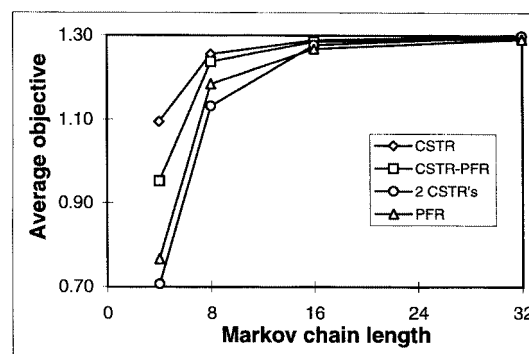

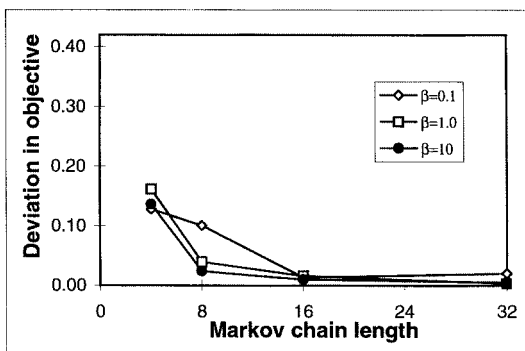
Figure 13. Study of initial states for Example 1 (i).
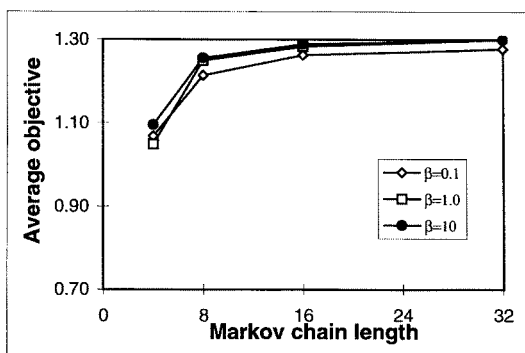
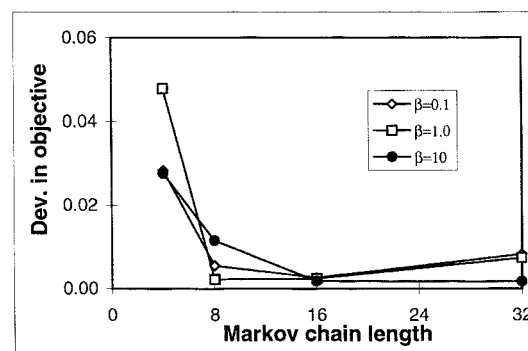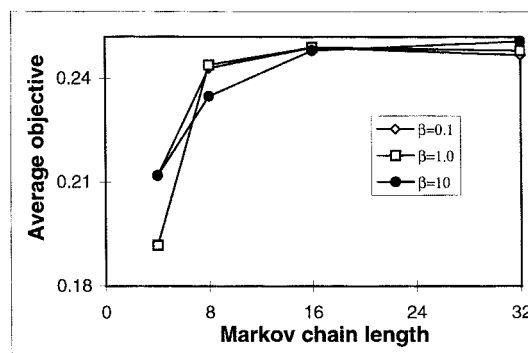Figure 14. Study of initial annealing temperatures for Example 1 (i).

Figure 15. Study of initial annealing temperatures for Example 1 (ii).

the targets remain unaffected by the initialization strategy, as the standard deviation of the stochastic experiments remains within $0.1 \div 1.0\%$ ($N = 32$) and $0.8 \div 1.4\%$ ($N = 16$). Figure 13b illustrates the spread on the deviation for each case.

The robustness of the targeting procedure with respect to its algorithmic parameters is presented in Figures 14a and 14b. Figure 14a illustrates the targets for different initial annealing temperatures, β^0. Unless they are for particularly small temperatures ($\beta^0 = 0.1$), the incremental gains in employing higher temperatures are small. Based on Figure 14a, targets for $\beta^0 = 1.0$ and $\beta^0 = 10.0$ change by 0.07%. The layout of standard deviations is presented in Figure 14b.

Figure 15 presents results similar to those in Figure 14, with respect to the second objective.

Screening and Scoping. Table 3 presents the designs obtained at $N = 32$, $\beta^0 = 10$ for maximum selectivity. The results indicate a single PFR as the optimal design (4 PFRs in series), with volume 19.7–21.3 lt. The cascade in the solution is apparently due to the low degree of discretization in the PFR (7 sub-CSTRs). The performance can be improved further by using conventional deterministic solvers and/or by employing more sub-CSTRs in the PFR representation. The final improvements have shifted the targets further to 1.319 (20.7 lt, 200 sub-CSTRs).

Table 3 also presents a list of designs for short chains ($N = 4$, $\beta^0 = 10$) and unconverged results ($N = 4$, $\beta^0 = 0.1$). Even for the case of unconverged runs, optimization results have come very close to the targets (S1, S2, S3). In other words, although the *average* performance illustrated on Figures 12a, 13a, 14a, and 15a is inferior to the targets, the *best* designs

reported from each stochastic experiment are within $\pm 3.1\%$ of the actual target.
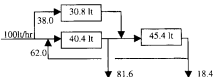
The designs reported in Table 4 apply to the conversion objective, and they follow a similar analysis. The initial guess is a CSTR with volume 5 lt and objective $9.051 \cdot 10^{-2}$ mol/lt. Deterministic optimization in the form of NLPs can be used to further improve the performance to 0.2573 mol/lt (39.4 lt, 200 sub-CSTRs).

Comparison with Results in the Literature. Similar optimization results are reported by groups that applied mathe-

Table 3. Selected Designs for Example 1 (i)

| Final Network Structures (7 Sub-CSTRs)	Selectivity of B over D
$\beta^0 = 10$, $N = 32$	
S1 4 PFR cascade [3.11, 5.19, 6.50, 5.46 lt]	1.304
S2 4 PFR cascade [5.74, 3.72, 6.60, 5.20 lt]	1.304
S3 4 PFR cascade [4.93, 4.90, 5.12, 4.76 lt]	1.304
$\beta^0 = 10$, $N = 4$	
S4 Single PFR (20.7 lt)	1.255
S5 Single PFR (18.1 lt)	1.252
S6 Single PFR (13.4 lt)	1.213
$\beta^0 = 0.1$, $N = 4$ (unconverged)	
S7 2 PFR cascade [1.65, 20.6 lt]; 60% feed bypass to second PFR; 20% bypass from first PFR to product	1.224
S8 CSTR–PFR (5.09, 10.7 lt) in parallel, 87% feed to PFR	1.140
S9 Single PFR (10.2 lt)	1.141

Table 4. Selected Designs for Example 1 (ii)

Final Network Structures (7 Sub-CSTRs)	Conversion B (mol/lt)
$\beta^0 = 10$ mol/lt, $N = 32$	
S1 3 PFRs–CSTR [10.9, 12.6, 12.6, 2.77 lt]	0.2528
S2 1 CSTR–3 PFRs [1.32, 10.2, 9.02, 19.7 lt]	0.2526
S3 3 PFR cascade [5.09, 12.6, 21.7 lt]	0.2519
$\beta^0 = 0.1$ mol/lt, $N = 4$ (unconverged)	
S4 2 PFR cascade [1.10, 63.3 lt]	0.2304
S5 PFR–CSTR (66.7, 3.60 lt) in series;	0.2183
CSTR features 23.5% interchange with	
a second CSTR (7.70 lt)	
S6	0.2009

(S6 diagram:)
100 lt/hr → 38.0 → 30.8 lt → 45.4 lt
62.0 → 40.4 lt
→ 81.6   → 18.4

matical programming (Kokossis and Floudas, 1990), though without the confidence for optimality as it is presented here. Unlike efforts to instill such confidence through combinations with graphical methods (Balakrishna and Biegler, 1992a), the optimization approach presented here has no need to integrate itself with these methods. Indeed, the approach can equally apply to the larger and more complicated problems of multiphase systems (Metha and Kokossis, 1998, 1999a,b).

Example 2: Van de Vusse reaction

The reaction scheme involves four components and is described by:

$$A \xrightarrow{1} B, \quad B \xrightarrow{2} C, \quad 2A \xrightarrow{3} D$$
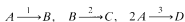
The kinetic vector assumes the form

$$\mathbf{R} = [R_1, R_2, R_3] = [-k_1 \cdot C_A, -k_2 \cdot C_B, -k_3 \cdot C_A^2],$$

where $k_1 = 10$ s^{-1}; $k_2 = 1.0$ s^{-1}; $k_3 = 0.5$ lt/mol·s. The feed flow rate is 100 lt/min and consists of pure A. The design objective is to maximize the outlet concentration of B, assuming feed concentrations $C_A^0 = 0.58$ mol/lt (Case A) and $C_A^0 = 5.8$ mol/lt (Case B). The different design stages are described as follows.

Targeting Stage. The maximum concentration of B is 0.4304 mol /lt for Case A and 3.661 mol/lt for Case B. Results for each stochastic run required 128 CPU·s for Case A and 157 CPU·s for Case B on the average. Statistical experiments included 10 runs. In all cases the optimization started from a single CSTR with a volume of 10^4 lt. Figures 16a and 17a illustrate targeting results against different Markov chains and initial annealing temperatures. The feed concentration sets an upper bound for the objective, thus affecting the values of β^0 employed. The results are again presented based on the *average values* of the stochastic experiments that are lower than the optimal values observed. As in the previous example, Markov chains longer than 16 account for satisfactory convergence. For such chains, σ is less than 0.74% (Case A) and 0.93% (Case B), as shown in Figures 16b and 17b.
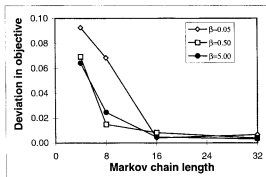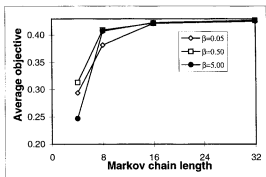

Figure 16. Results for Example 2: Case A.

Screening and Scoping. Tables 5 (Case A) and 6 (Case B) present the designs obtained at $N = 32$, $\beta^0 = 5.0$, and 50 mol/lt, respectively. For Case A, the initial guess is a CSTR (volume 10^4 lt, objective 5.765×10^{-3} mol/lt). The designs
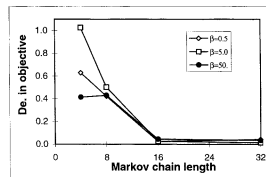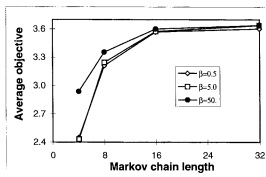

Figure 17. Results for Example 2: Case B.

Table 5. Selected Designs for Example 2: Case *A*

	Final Network Structures, $\beta^0 = 5.0$ mol/lt, $N = 32$ (7 Sub-CSTR)	Conversion B (mol/lt)
S1	3 PFR cascade [10.8, 4.54, 11.1 lt]	0.4304
S2	1 CSTR and 3 PFRs cascade [1.45, 6.48, 8.90, 9.84 lt]	0.4299
S3	3 PFR cascade [4.93, 6.45, 13.7 lt]	0.4295
S4	4 PFRs in series [0.240, 11.5, 1.48, 14.5 lt]; 76% feed bypass to second PFR	0.4285
S5	3 PFRs in series [14.7, 8.88, 5.39 lt]; third PFR features 7.3% recycle	0.4284

(S1, S3, S4, and S5) of Table 5 clearly suggest the PFR as the optimal structure (25.1–29.0 lt). As in Example 1, the cascades only reflect on the low discretization employed for the plug flow (7 sub-CSTRs/PFR). Design S2 also suggests a single PFR, as the design employs a CSTR that is similar in size (1.45 lt) to the sub-CSTRs of the PFR representation (0.93-1.41 lt). For Case *B*, the initial guess is a CSTR (volume 10^4 lt, objective 5.734×10^{-2} mol/lt). The designs of Table 6 include CSTR–PFR structures (S1–S4) and a single PFR (S5). The CSTR volumes fall within 10.5–12.0 lt and the PFR volumes within 17.3–18.4 lt (except S5).

It is important to note that a higher degree of discretization for the plug flow is always possible but meaningless. Indeed, the authors highly discourage this practice. Once the most difficult part of screening is accomplished with the use of stochastic optimization, further and easy improvements can be achieved by using deterministic optimization solvers and/or by making improvements in the representation of the plug flow. For example, such improvements can further increase the target behind S1 (Table 5) to 0.4364 mol/lt (+1.4%) and the target for S1 (Table 6) to 3.680 (+0.52%). The PFR (Case *A*) and the CSTR–PFR (Case *B*) schemes have been previously reported in the literature (Glasser et al., 1987; Kokossis and Floudas, 1990).

Example 3: A polynomial test of kinetics

In the previous example, it is claimed that simple representations for the plug flow are adequate, as the approach can be combined with better models once the screening is completed. In order to further illustrate the point, a more challenging example is selected where highly nonlinear kinetics are involved. The example is a contrived problem presented by Glasser et al. (1987) to illustrate the efficiency of graphical methods. The reaction involves two key components with kinetics given by:

$$\boldsymbol{R} = [\, R_X, R_Y \,] = \left[\, x \cdot F(x),\ F(x)^2 + x \cdot F'(x) \cdot y \,\right];$$

$$x = C_A/C_A^0; \quad y = C_B/C_A^0,$$

where the functions $F(x)$ and $F'(x)$ follow polynomial expressions based on x:

$$F(x) = 6 \cdot x^6 - 6 \cdot x^5 + 9 \cdot x^4 - 16 \cdot x^3 + 9 \cdot x^2 - 2 \cdot x \quad \text{and}$$

$$F'(x) = dF(x)/dx$$

The feed flow rate is 100 lt/h, and consists of pure A ($x^0 = 1$, $y^0 = 0$). The objective is to maximize the concentration of product B in the effluent stream. The PFR is again presented by 7 sub-CSTRs.

Targeting Stage. The maximum value of y is 65.35%. Stochastic runs carried out for different initial guesses and algorithmic parameters indicate a need for longer Markov chains, compared to the length used in conventional problems. Statistical experiments are carried out at $N = 110$, $\beta^0 = 1.0$, starting from different initial structures. The experiments include 15 runs and result in an average objective of 62.72% and σ of 1.56%.

Screening and Scoping. Table 7 summarizes the results obtained at $N = 110$, $\beta^0 = 1.0$, starting from different initial guesses, namely a single CSTR, a single PRF, and 4 CSTRs in series. The results include several, equally promising designs that suggest the CSTR–PFR–CSTR–PFR structure reported by Glasser et al. (1987), along with other similar arrangements that include bypasses (S6, S8, S15), interchanges (S10, S12), and recycles (S11, S13, S14). Structures S7, S9, and S13 feature a CSTR–PFR–CSTR arrangement. At this stage, an increase in the sub-CSTRs in the representation of the plug flow and the use of mathematical programming can further improve the performance from 65% (7 sub-CSTRs) to 68% (200 sub-CSTRs). Similar gains can be found for the other final designs. Designs featuring the sequence of CSTR–PFR–CSTR can reach a performance of 67% (200 sub-CSTRs) starting from 61–63% (7 sub-CSTRs). In brief, even for a more complex problem, the use of a simpler representation has retained the screening functions of the approach and justified the overall development from targets to designs. It is evident that mathematical-programming approaches have no chance of handling the type of kinetics reported here, while the graphical methods are limited in extending their analysis to higher dimensions. The proposed approach requires no adjustments to the overall procedure, and the same, simple representations can be used without a loss of optimality.
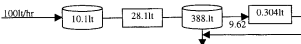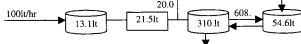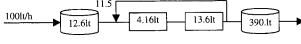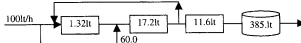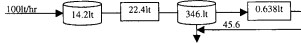
Example 4: Design of a bifurcational catalyst for benzene production

An isomerization and a hydrogenation component are used in a bifunctional catalyst to produce benzene from methylcyclopentane (Luus et al., 1991). The catalyst consists of an isomerization component and a hydrogenation component. The

Table 6. Selected Designs for Example 2: Case *B*

	Final Network Structures, $\beta^0 = 50$ mol/lt, $N = 32$ (7 Sub-CSTRs)	Conversion B (mol/lt)
S1	CSTR–3 PFRs [11.6, 7.13, 4.20, 6.07 lt]	3.661
S2	CSTR–3 PFRs [10.7, 5.65, 5.48, 6.47 lt]; 6.8% recycle first PFR to CSTR	3.659
S3	CSTR–3 PFRs [10.5, 4.91, 5.85, 7.65 lt]; 25% recycle first PFR to CSTR	3.656
S4	CSTR–PFR (12.0, 17.3 lt) in series	3.621
S5	Single PFR (26.8 lt)	3.550

Table 7. Selected Designs for Example 3

Final Network Structures, $\beta^0 = 1.0$, $N = 110$ (7 Sub-CSTRs)	y (%)
S1 CSTR–PFR–CSTR–PFR [11.0, 30.3, 372., 38.9 lt]	65.35
S2 CSTR–PFR–CSTR–PFR [10.9, 28.5, 382., 38.2 lt]	65.28
S3 CSTR–PFR–CSTR–PFR [12.8, 20.6, 371., 45.2 lt]	63.99
S4 CSTR–PFR–CSTR–PFR [10.8, 24.9, 411., 37.0 lt]	63.82
S5 CSTR–PFR–CSTR–PFR [11.1, 21.8, 412., 34.6 lt]	63.40
S6	63.28
S7 CSTR–CSTR–PFR–CSTR [11.3, 3.63, 22.9, 381. lt]	62.92
S8	62.83
S9 CSTR–PFR–PFR–CSTR [12.0, 18.0, 4.66, 383 lt]	62.57
S10	62.13
S11	62.07
S12	61.50
S13	60.96
S14	60.32
S15	60.32

S6: 100 lt/h → 6.83 lt → 18.8 lt → 13.2 lt → 382. lt (recycle 40.0)

S8: 100 lt/hr → 10.1 lt → 28.1 lt → 388. lt → 0.304 lt (9.62)

S10: 100 lt/h → 11.4 lt → 23.1 lt → 391. lt ⇄ 5.96 lt (400)

S11: 100 lt/hr → 14.7 lt → 1.67 lt → 19.2 lt → 396. lt (recycle 66.7)

S12: 100 lt/h → 13.1 lt → 21.5 lt → 310. lt → 54.6 lt (20.0, 608.)

S13: 100 lt/h → 12.6 lt → 4.16 lt → 13.6 lt → 390. lt (11.5)

S14: 100 lt/h → 1.32 lt → 17.2 lt → 11.6 lt → 385. lt (60.0)

S15: 100 lt/h → 14.2 lt → 22.4 lt → 346. lt → 0.638 lt (45.6)

---

reaction scheme is described by:
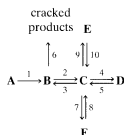
where **A**: methylcyclopentane; **B**: methycyclopentene; **C**: cyclohexene; **D**: benzene; **E**: cyclohexane; **F**: toluene. The reactions are first order and proceed isothermally. The kinetic constants are cubic functions of the catalyst blend (u): $k_j = \sum_{n=0}^{3} \alpha_{j,n} \cdot u^n$, $\forall j = 1, \ldots, 10$, with u defined as the mass fraction of the hydrogenation component over the total catalyst mass. Table 8 provides the values of $\alpha_{j,n}$, and the objective is to determine the profile of u that maximizes the effluent

concentration of benzene along a PFR with residence time 2,000 g·h/mol. The PFR consists of 10 segments (5 sub-CSTRs/segment) of different catalyst blends. The catalyst blend varies within 0.6–0.9, and the feed flow rate is 100 lt/h and consists of pure methylcyclopentane (1 mol/lt).

Targeting Stage. The results are summarized in Figure 18. Moves allow changes to the compositions, u_i, of the catalyst blend in each PFR segment, i. The additional move for u is achieved with a discretization of u_i by a 1% increment, and employs a uniform probability distribution. The maximum concentration of benzene is 10.05×10^{-3} mol/lt. Statistical experiments each included 5–15 runs, and initial annealing temperatures ranged from 2.0×10^{-3} mol/lt to 20×10^{-3} mol/lt. For chains longer than 30, σ has been less than 0.6%.

Screening and Scoping. Table 9 presents the solutions obtained for $N = 40$, $\beta^0 = 20 \times 10^{-3}$ mol/lt. The initial value for all the u_i is 0.6, resulting in an objective of 5.463×10^{-3} mol/lt (5 sub-CSTRs per PFR segment). Solutions S1, S2, and S3 feature maximum hydrogenation compositions ($u = 0.90$) from the fourth PFR segments and result in maximum

Table 8. Kinetic Parameters for Example 4

Reaction (j)	$\alpha_{j,1}$	$\alpha_{j,2}$	$\alpha_{j,3}$	$\alpha_{j,4}$
1	0.2918487×10^{-2}	$-0.8045787 \times 10^{-2}$	0.6749947×10^{-2}	$-0.1416647 \times 10^{-2}$
2	0.2682093×10^{2}	-0.9556079×10^{2}	0.1130398×10^{3}	-0.3166655×10^{3}
3	0.2087241×10^{3}	-0.7198052×10^{3}	0.8277466×10^{3}	-0.4429997×10^{2}
4	-0.3950534	0.1679353×10^{1}	-0.1777829×10^{1}	0.4974987
5	$-0.2504665 \times 10^{-4}$	0.1005854×10^{-1}	$-0.1986696 \times 10^{-1}$	0.9833470×10^{-2}
6	0.9509977×10^{1}	-0.3500994×10^{2}	0.4283329×10^{2}	-0.1733333×10^{2}
7	0.1350005×10^{1}	-0.6850027×10^{1}	0.1216671×10^{2}	-0.6666689×10^{1}
8	0.1921995×10^{-1}	$-0.7945320 \times 10^{-1}$	0.1105666	$-0.5033333 \times 10^{-1}$
9	0.1323596	-0.4696255	0.5539323	-0.2166664
10	0.7339981×10^{1}	-0.2527328×10^{2}	0.2993329×10^{2}	-0.1199999×10^{2}

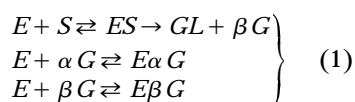**Table 9. Selected u-Profiles for Example 4**

	Final Catalyst Compositions in PFR Segments, $\beta^0 = 20.10^{-3}$ mol/lt, $N = 40$										Benzene (10^3 mol/g)
	1st	2nd	3rd	4th	5th	6th	7th	8th	9th	10th	
S1	0.666	0.673	0.677	0.900	0.900	0.900	0.900	0.900	0.900	0.900	10.050
S2	0.671	0.691	0.676	0.900	0.900	0.900	0.900	0.900	0.900	0.900	10.030
S3	0.666	0.655	0.672	0.900	0.900	0.900	0.900	0.900	0.900	0.900	10.026
S4	0.668	0.676	0.681	0.682	0.900	0.900	0.900	0.900	0.900	0.900	9.9890
S5	0.669	0.672	0.680	0.679	0.900	0.900	0.900	0.900	0.900	0.900	9.9889
S6	0.668	0.678	0.677	0.683	0.900	0.900	0.900	0.900	0.900	0.900	9.9886
S7	0.672	0.675	0.682	0.678	0.900	0.900	0.900	0.900	0.900	0.900	9.9877

performances ($10.026 - 10.050 \times 10^{-3}$ mol/lt). Solutions S3 to S7 feature instead the maximum compositions from the fifth segment and result in a lower overall performance ($9.9877 - 9.9890 \times 10^{-3}$ mol/lt). The optimal profiles are similar to the results of Luus et al. (1991), who studied the problem using dynamic programming and analysis. The use of the stochastic tool results in no measurable difference between the best solution (10.050×10^{-3} mol/lt) and the worst (9.9877×10^{-3} mol/lt).

Example 5: Hydrolysis of lactose by β-galactosidase

The reaction mechanism (Bakken et al., 1989; Bailey and Ollis, 1986) is given by

$$
\left.
\begin{aligned}
E + S &\rightleftarrows ES \rightarrow GL + \beta G \\
E + \alpha G &\rightleftarrows E\alpha G \\
E + \beta G &\rightleftarrows E\beta G
\end{aligned}
\right\} \quad (1)
$$

$$\beta G \rightleftarrows \alpha G \qquad (2)$$

$$GL \rightarrow GA \qquad (3)$$

$$E \rightarrow Ed, \qquad (4)$$

where E: enzyme; S: substrate (lactose); G: galactose (α, β forms); Ed: deactivated enzyme; GL: glucose; GA: gluconic acid. The kinetic expressions take the form

$$\Re_1 = C_E \cdot C_S \cdot \left[1 + C_{\alpha G}/K_{\alpha G} + C_{\beta G}/K_{\beta G} \right]^{-1},$$

$$K_{\alpha G} = 0.003, \ K_{\beta G} = 0.079$$

$$\Re_2 = 50 \cdot (C^*_{\alpha G} - C_{\alpha G}),$$

$$C^*_{\alpha G} = \left(C^0_S + C^0_{\alpha G} + C^0_{\beta G} - C_S \right) \cdot K/(K+1), \ K = 0.1111$$

$$\Re_3 = 0.083 \cdot C_{GL}, \qquad \Re_4 = 0.047 \cdot C_E$$

The objective is to maximize the concentration of glucose for a feed stream of 100 lt/min that consists of 100.0 mol/lt lactose, 0.65 mol/lt β-galactosidase, and traces of galactose (0.001 mol/lt for each form).

Targeting Stage. The maximum conversion of glucose is 2.7 mol/lt. Results for each stochastic run require 860 CPU·s on the average, and statistical analysis is based on 10 runs. The
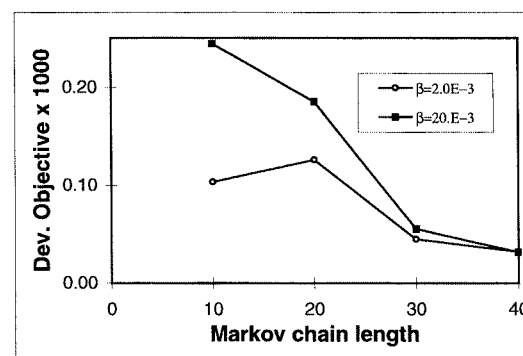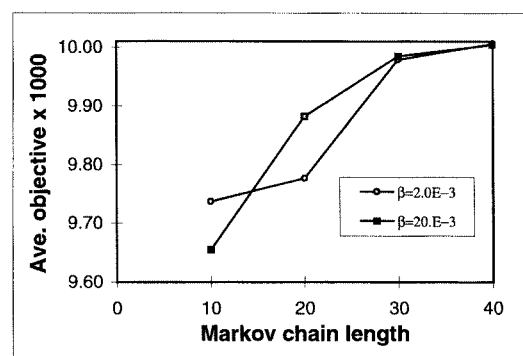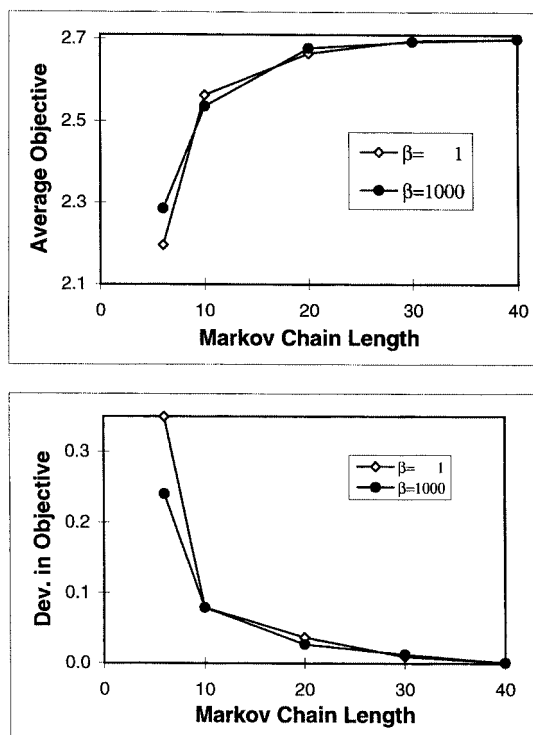

Figure 18. Results for Example 4.

Figure 19. Results for Example 5.

Conclusions

This article presents a new synthesis approach that applies optimization technology to the design of chemical reactors. As the first stage, the approach calculates reliable targets for the performance of a reaction system. The development of targets is followed by a proposed solution set comprising simple and complex combinations of reactors that perform close to the targets. Confidence levels are calculated to assess the quality of the targets using stochastic optimization techniques and simulated annealing.

From a practical viewpoint, the approach can be used to evaluate the operation of new and existing reactors. New reactors can be developed so that they match the targets and follow one or more of the layouts selected in the optimization. The performance of existing reactors can be compared with the targets and the incentives for modifying their operation determined. Ideas for changing them can be obtained by reviewing the list of available designs and adjusting the reactor's performance to achieve the characteristics of the selected options.

The methodology is not limited by the typical complexities of the reactor models or the reaction kinetics. Its implementation has proved to be robust enough to encourage applications in larger and more complicated systems. Indeed, research is already in progress for reaction systems with more than a single phase (Mehta and Kokossis, 1997a,b,c,d,e,f, 1998), and subsequent articles address a systematic way of extending these developments (Mehta and Kokossis, 1999a,b,c).

initial guess is 2 CSTRs with feed bypass, leading to an initial objective 0.5247 mol/lt. Figures 19a and 19b present the development of the average and the standard deviation for different initial annealing temperatures, and different Markov chains. Deviations at chain lengths greater than $N = 40$ fall below 0.04%.

Screen and Scoping. Table 10 presents final designs at ($N = 20$, $\beta = 1,000$ mol/lt), starting from different initial states, namely 4 CSTR cascade, 4 PFR cascade, and 2 CSTRs with feed bypass. The results suggest a single PFR (PFR cascade) with a volume of 731−763 lt. Stochastic results of 2.7 mol/lt (7 sub-CSTRs) can be improved to 2.744 mol/lt (50 sub-CSTRs), with a PFR volume of 750 lt, using NLP technology.

Table 10. Selected Designs for Example 5

Final Network Structure, $\beta^0 = 10^3$ mol/lt, $N = 20$ (7 Sub-CSTRs)		Vol. (lt)	Lactose (kmol/lt)
S1	4 PFR cascade	762.0	2.7000
S2	4 PFR cascade	741.0	2.6999
S3	4 PFR cascade	761.0	2.6996
S4	4 PFR cascade	731.0	2.6995
S5	4 PFR cascade	754.0	2.6976
S6	4 PFR cascade	761.0	2.6956
S7	4 PFR cascade	749.0	2.6946
S8	4 PFR cascade	752.0	2.6872
S9	4 PFR cascade	743.0	2.6846
S10	4 PFR cascade	723.0	6.6793
S11	4 PFR cascade	763.0	6.6778
S12	4 PFR cascade	752.0	2.6775

Literature Cited

Aarts, E. H. L., and P. G. M. van Laarhoven, "Statistical Cooling: A General Approach to Combinatorial Optimization Problems," *Philips J. Res.*, **40**, 193 (1985).

Achenie, L. E. K., and L. T. Biegler, "Algorithmic Synthesis of Chemical Reactor Networks Using Mathematical Programming," *Ind. Eng. Chem. Fundam.*, **25**, 621 (1986).

Achenie, L. E. K., and L. T. Biegler, "Developing Targets for the Performance Index of a Reactor Network," *Ind. Eng. Chem. Res.*, **27**, 1811 (1988).

Achenie, L. E. K., and L. T. Biegler, "A Superstructure Based Approach to Chemical Reactor Network Synthesis," *Comput. Chem. Eng.*, **14**, 23 (1990).

Aris, R., "Studies in Optimisation. III. The Optimum Operating Conditions in Sequences of Stirred Tank Reactors," *Chem. Eng. Sci.*, **13**, 75 (1960).

Aris, R., "Studies in Optimisation—IV. The Optimum Conditions for a Single Reaction," *Chem. Eng. Sci.*, **13**, 197 (1961).

Athier, G., P. Floquet, L. Pibouleau, and S. Domenech, "Process Optimization by Simulated Annealing and NLP Procedures. Application to Heat Exchanger Network Synthesis," *Comput. Chem. Eng.*, **21**, S475 (1997a).

Athier, G., P. Floquet, L. Pibouleau, and S. Domenech, "Synthesis of Heat-Exchanger Network by Simulated Annealing and NLP Procedures," *AIChE J.*, **43**, 3007 (1997b).

Athier, G., P. Floquet, L. Pibouleau, and S. Domenech, "A Mixed

Method for Retrofitting Heat Exchanger Networks," *Comput. Chem. Eng.*, **22**, S505 (1998).

Bailey, D. F., and D. F. Ollis, *Biochemical Engineering Fundamentals*, 2nd ed., McGraw-Hill, New York (1986).

Bakken, A. P., C. G. Hill, Jr., and C. H. Amundson, "Hydrolysis of Lactose in Skim Milk by Immobilized β-Galactosidase in a Spiral Flow Reactor," *Biotechnol. Bioeng.*, **33**, 1249 (1989).

Balakrishna, S., and L. T. Biegler, "Constructive Targeting Approaches to the Synthesis of Chemical Reactor Networks," *Ind. Eng. Chem. Res.*, **31**, 300 (1992a).

Balakrishna, S., and L. T. Biegler, "Targeting Strategies for the Synthesis and Energy Integration of Nonisothermal Reactor Networks," *Ind. Eng. Chem. Res.*, **31**, 2152 (1992b).

Briones, V., and A. Kokossis, "A New Approach for the Optimal Retrofit of Heat Exchanger Networks," *Comput. Chem. Eng.*, **20**, S43 (1996).

Briones, V., and A. Kokossis, "Hypertarget: A Conceptual Programming Approach for the Optimisation of Industrial Heat Exchanger Networks: I. Grassroot Design," *Chem. Eng. Sci.*, **54**, 519 (1999a).

Briones, V., and A. Kokossis, "Hypertarget: A Conceptual Programming Approach for the Optimisation of Industrial Heat Exchanger Networks: II. Retrofit Design," *Chem. Eng. Sci.*, **54**, 541 (1999b).

Briones, V., and A. Kokossis, "Hypertarget: A Conceptual Programming Approach for the Optimisation of Industrial Heat Exchanger Networks: III. Industrial Applications," *Chem. Eng. Sci.*, **54**, 685 (1999c).

Chaudhuri, P. D., and U. M. Diwekar, "Process Synthesis Under Uncertainty: A Penalty Function Approach," *AIChE J.*, **42**, 742 (1996).

Chaudhuri, P. D., and U. M. Diwekar, "Synthesis Under Uncertainty with Simulators," *Comput. Chem. Eng.*, **21**, 733 (1997).

Chen, H. S., and M. A. Stadtherr, "A Modification of Powell's Dogleg Method for Solving Systems of Nonlinear Equations," *Comput. Chem. Eng.*, **5**, 143 (1981).

Chitra, S. P., and R. Govind, "Yield Optimization for Complex Reaction Systems," *Chem. Eng. Sci.*, **36**, 1219 (1981).

Chitra, S. P., and R. Govind, "Synthesis of Optimal Serial Reactor Structures for Homogeneous Reactions. Part I: Isothermal Reactors," *AIChE J.*, **31**, 177 (1985a).

Chitra, S. P., and R. Govind, "Synthesis of Optimal Serial Reactor Structures for Homogeneous Reactions. Part II: Nonisothermal Reactors," *AIChE J.*, **31**, 185 (1985b).

Cordero, J. C., A. Davin, P. Floquet, L. Pibouleau, and S. Domenech, "Synthesis of Optimal Reactor Networks Using Mathematical Programming and Simulated Annealing," *Comput. Chem. Eng.*, **21**, S47 (1997).

Das, H., P. T. Cummings, and M. D. LeVan, "Scheduling of Serial Multiproduct Batch Processes Via Simulated Annealing," *Comput. Chem. Eng.*, **14**, 1351 (1990).

Dolan, W. B., P. T. Cummings, and M. D. LeVan, "Heat Exchanger Network Design by Simulated Annealing," *Foundations of Computer-Aided Process Operations*, G. V. Reklaitis and H. D. Spriggs, eds., Elsevier, New York, p. 639 (1987).

Dolan, W. B., P. T. Cummings, and M. D. LeVan, "Process Optimization Via Simulated Annealing: Application to Network Design," *AIChE J.*, **35**, 725 (1989).

Dolan, W. B., P. T. Cummings, and M. D. LeVan, "Algorithmic Efficiency of Simulated Annealing for Heat Exchanger Networks," *Comput. Chem. Eng.*, **14**, 1039 (1990).

Dyson, D. C., and J. M. Horn, "Optimum Distributed Feed Reactors for Exothermic Reversible Reactions," *J. Optimiz. Theory Appl.*, **1**, 40 (1967).

Dyson, D. C., and J. M. Horn, "Optimum Adiabatic Cascade Reactor with Direct Intercooling," *Ind. Eng. Chem. Fundam.*, **8**, 49 (1969).

Feinberg, M., and D. Hildebrandt, "Optimal Reactor Design from a Geometric Viewpoint: I. Universal Properties of the Attainable Region," *Chem. Eng. Sci.*, **52**, 1637 (1997).

Floquet, P., L. Pibouleau, and S. Domenech, "Separation Sequence Synthesis: How to Use Simulated Annealing Procedure?," *Comput. Chem. Eng.*, **18**, 1141 (1994).

Gidas, B., "Nonstationary Markov Chains and Convergence of the Annealing Algorithm," *J. Stat. Phys.*, **39**, 73 (1985).

Glasser, B., D. Hildebrandt, and D. Glasser, "Optimal Mixing for Exothermic Reversible Reactions," *Ind. Eng. Chem. Res.*, **31**, 1541 (1992).

Glasser, D., and D. Hildebrandt, "Reactor and Process Synthesis," *Comput. Chem. Eng.*, **21**, S775 (1997).

Glasser, D., D. Hildebrandt, and C. M. Crowe, "A Geometric Approach to Steady Flow Reactors: The Attainable Region and Optimization in the Concentration Space," *Ind. Eng. Chem. Res.*, **26**, 1803 (1987).

Glasser, D., D. Hildebrandt, and S. Godorr, "The Attainable Region for Segregated Maximum Mixed and Other Reactor Models," *Ind. Eng. Chem. Res.*, **33**, 1136 (1994).

Godorr, S., D. Hildebrandt, D. Glasser, and C. McGregor, "Choosing Optimal Control Policies Using the Attainable Region Approach," *Ind. Eng. Chem. Res.*, **38**, 639 (1999).

Grossmann, I. E., "Mixed-Integer Programming Approach for the Synthesis of Integrated Process Flowsheets," *Comput. Chem. Eng.*, **9**, 463 (1985).

Hildebrandt, D., and L. T. Biegler, "Synthesis of Chemical Reactor Networks," *FOCAPD*, Snowmass, CO (1994).

Hildebrandt, D., and D. Glasser, "The Attainable Region and Optimal Reactor Structures," *Chem. Eng. Sci.*, **45**, 2161 (1990).

Hildebrandt, D., D. Glasser, and C. M. Crowe, "Geometry of the Attainable Region Generated by Reaction and Mixing: With and Without Constraints," *Ind. Eng. Chem. Res.*, **29**, 49 (1990).

Horn, F., "Attainable and Non-Attainable Regions in Chemical Reaction Technique," *Proc. Euro. Symp. on Chemical Reaction Engineering*, Pergamon Press, London (1964).

Hopley, F., D. Hildebrandt, and D. Glasser, "Optimal Reactor Structures for Exothermic Reversible-Reactions with Complex kinetics," *Chem. Eng. Sci.*, **51**, 2399 (1996).

Jackson, R., "Optimization of Chemical Reactors with Respect to Flow Configuration," *J. Optimiz. Theory Appl.*, **2**, 240 (1968).

Johnson, N. L., and S. Kotz, *Distributions in Statistics: Continuous Univariate Distributions*, Vol. 1, *The Houghton Mifflin Series in Statistics*, H. Chernoff, ed., Houghton Mifflin, Boston (1970).

Kelkar, V. V., and K. M. Ng, "Screening Procedure for Synthesizing Isothermal Multiphase Reactors," *AIChE J.*, **44**, 1563 (1998).

Kirkpatrick, S., C. D. Gelatt, Jr., and M. P. Vecchi, "Optimization by Simulated Annealing," *Science*, **220**, 671 (1983).

Kokossis, A. C., and C. A. Floudas, "Optimization of Complex Reactor Networks: I. Isothermal Operation," *Chem. Eng. Sci.*, **45**, 595 (1990).

Kokossis, A. C., and C. A. Floudas, "Synthesis and Optimization of Isothermal Reactor Separator Recycle Systems," *Chem. Eng. Sci.*, **46**, 261 (1991).

Kokossis, A. C., and C. A. Floudas, "Optimization of Complex Reactor Networks: II. Nonisothermal Operation," *Chem. Eng. Sci.*, **49**, 1037 (1994).

Lakshmanan, A., and L. T. Biegler, "Reactor Network Targeting for Waste Minimization," *Pollution Prevention via Process and Product Modifications, AIChE Symp. Ser. 90*, M. El-Halwagi and D. Petrides, eds., AIChE, New York, p. 128 (1994).

Lakshmanan, A., and L. T. Biegler, "Synthesis of Optimal Chemical Reactor Networks," *Ind. Eng. Chem. Res.*, **35**, 1344 (1996).

Lakshmanan, A., and L. T. Biegler, "A Case Study for Reactor Network Synthesis: The Vinyl Chloride Process," *Comput. Chem. Eng.*, **21**, S785 (1997).

Levenspiel, O, *Chemical Reactor Engineering. An Introduction to the Design of Chemical Reactors*, Wiley, New York (1962).

Luus, R., J. Dittrich, and F. J. Keil, "Multiplicity of Solutions in the Optimization of a Bifunctional Catalyst Blend in Tubular Reactor," AIChE Meeting, Los Angeles (1991).

Maia, L. O. A., L. A. Vidal de Carvalho, and R. Y. Qassim, "Synthesis of Utility Systems by Simulated Annealing," *Comput. Chem. Eng.*, **19**, 481 (1985).

Marcoulaki, E. C., and A. C. Kokossis, "Reactor Network Synthesis Using Stochastic Optimization Methods," *1995 Inst. Chem. Eng. Res. Event*, **1**, 113 (1995).

Marcoulaki, E. C., and A. C. Kokossis, "Design of Chemical Reactor Networks Using Stochastic Optimisation Methods," AIChE Meeting, New Orleans (1996a).

Marcoulaki, E. C., and A. C. Kokossis, "Stochastic Optimisation of Complex Reactor Systems," *Comput. Chem. Eng.*, **20**, S231 (1996b).

Marcoulaki, E. C., and A. C. Kokossis, "Molecular Design Synthesis

Using Stochastic Optimisation as a Tool for Scoping and Screening," *Comput. Chem. Eng.*, **22**, S11 (1998).

McGregor, C., D. Glasser, and D. Hildebrandt, "The Attainable Region and Pontryagin's Maximum Principle," *Ind. Eng. Chem. Res.*, **38**, 652 (1999).

Mehta, V., and A. Kokossis, "Development of Novel Multiphase Reactors Using a Systematic Design Framework," *Comput. Chem. Eng.*, **21**, S325 (1997a).

Mehta, V., and A. Kokossis, "New Generation Tools for Multiphase Chemical Reactors: A Systematic Methodology for Novelty and Design Automation," AIChE Meeting, Los Angeles (1997b).

Mehta, V., and A. Kokossis, "Synthesis of Membrane and Reactive Separation Networks Using Integrated Optimisation Systems," AIChE Meeting, Los Angeles (1997c).

Mehta, V., and A. Kokossis, "Reactor Designs for the Propylene Ammoxidation to Acrylonitrile: Targeting, Scoping and Screening Using a Systematic Approach," AIChE Meeting, Los Angeles (1997d).

Mehta, V., and A. Kokossis, "New Generation Tools for Multiphase Chemical Reactors: Reactor Design, Targeting, Scoping and Screening for the Chlorination of Butanoic Acid Using a Systematic Approach," AIChE Meeting, Los Angeles (1997e).

Mehta, V., and A. Kokossis, "New Generation Tools for Multiphase Chemical Reactors: A Systematic Methodology for Novelty and Design Automation," AIChE Meeting, Los Angeles (1997f).

Mehta, V., and A. Kokossis, "New Generation Tools for Multiphase Reaction Systems: A Validated, Systematic Methodology for Novelty and Design Automation," *Comput. Chem. Eng.*, **22**, S119 (1998).

Mehta, V., and A. Kokossis, "Multiphase Reactor Network Synthesis and Optimisation: I. The Shadow Reactor Superstructure," *Chem. Eng. Sci.*, in press (1999a).

Mehta, V., and A. Kokossis, "Multiphase Reactor Network Synthesis and Optimisation: II. The Optimisation Framework," *Chem. Eng. Sci.*, in press (1999b).

Mehta, V., and A. Kokossis, "Optimisation of Nonisothermal Multiphase Reactors," *AIChE J.*, , in press (1999c).

Metropolis, N., A. W. Rosenbluth, M. N. Rosenbluth, A. H. Teller, and E. Teller, "Equation of State Calculations for Fast Computing Machines," *J. Chem. Phys.*, **21**, 1087 (1953).

Muller, F. U., and A. C. Kokossis, "Integration of Targeting and Stochastic Optimization for Heat Exchanger Network Synthesis," *1995 Inst. Chem. Eng. Res. Event*, **1**, 71 (1995).

Ng, D. Y. C., and D. W. T. Rippin, "The Effect of Incomplete Mixing on Conversion in Homogeneous Reactions," *Proc. Euro. Symp. on Chemical Reaction Engineering*, Pergamon Press, Oxford (1965).

Nisoli, A., M. F. Malone, and M. F. Doherty, "Attainable Regions for Reaction with Separation," *AIChE J.*, **43**, 374 (1997).

Nielsen, J., V. Briones, and A. C. Kokossis, "An Integrated Framework for the Optimal Design of Heat Recovery Systems," AIChE Meeting, San Francisco (1994).

Painton, L. A., and U. M. Diwekar, "Stochastic Annealing for Synthesis Under Uncertainty," *Eur. J. Oper. Res.*, **83**, 489 (1995).

Patel, A. N., R. S. H. Mah., and I. A. Karimi, "Preliminary Design of Multiproduct Noncontinuous Plants Using Simulated Annealing," *Comput. Chem. Eng.*, **15**, 451 (1991).

Paynter, J. D., and D. E. Haskins, "Determination of Optimal Reactor Type," *Chem. Eng. Sci.*, **25**, 1415 (1970).

Price, J. G., D. Glasser, D. Hildebrandt, and N. J. Coville, "Fischer-Tropsch Synthesis: DRIFTS and SIMS Surface Investigation of Co and Co/Ru on Titania Supports," *Stud. Surf. Sci. Catal.*, **107**, 243 (1997).

Ravimohan, A. L., "Optimization of Chemical Reactor Networks with Respect to Flow Configuration," *J. Optimiz. Theory Appl.*, **8**, 204 (1971).

Rojnuckarin, A., C. A. Floudas, H. Rabitz, and R. A. Yetter, "Methane Conversion to Ethylene and Acetylene: Optimal Control with Chlorine, Oxygen, and Heat Flux," *Ind. Eng. Chem. Res.*, **35**, 683 (1996).

Schweiger, C. A., and C. A. Floudas, "Optimization Framework for the Synthesis of Chemical Reactor Networks," *Ind. Eng. Chem. Res.*, **38**, 744 (1999).

Shah, B. S., and A. Kokossis, "Design Targets of Separator and Reactor-Separator Systems Using Conceptual Programming," *Comput. Chem. Eng.*, **21**, S1013 (1997).

Sorkin, G. B., "Efficient Simulated Annealing on Fractal Energy Landscapes," *Algorithmica*, **6**, 367 (1991).

Xia, Q., and S. Macchietto, "Design and Synthesis of Batch Plants—MINLP Solution Based on a Stochastic Method," *Comput. Chem. Eng.*, **21**, S697 (1997).